



# Low-temperature sintered $\text{Zn}_2\text{SiO}_4$ – $\text{CaTiO}_3$ ceramics with near-zero temperature coefficient of resonant frequency

Gang Dou<sup>a</sup>, Dongxiang Zhou<sup>a,\*</sup>, Mei Guo<sup>a,b</sup>, Shuping Gong<sup>a</sup>

<sup>a</sup> Department of Electronic Science and Technology, Huazhong University of Science and Technology, Wuhan 430074, PR China

<sup>b</sup> Department of Materials Science and Engineering, The University of Sheffield, Mappin Street, Sheffield S1 3JD, United Kingdom

## ARTICLE INFO

### Article history:

Received 22 June 2011

Received in revised form 21 October 2011

Accepted 24 October 2011

Available online 10 November 2011

### Keywords:

LTCC

Microwave dielectric properties

$\text{Zn}_2\text{SiO}_4$ – $\text{CaTiO}_3$

$\text{Li}_2\text{CO}_3$

$\text{H}_3\text{BO}_3$

## ABSTRACT

The microwave dielectric properties and the microstructures of  $(1-x)\text{Zn}_2\text{SiO}_4-x\text{CaTiO}_3$  composite ceramics with  $\text{Li}_2\text{CO}_3$ – $\text{H}_3\text{BO}_3$  additives prepared by solid-state reaction method have been investigated. The crystalline phases were studied systematically by using the X-ray diffraction (XRD), microstructures by the scanning electron microscopy (SEM) and composition analysis by energy-dispersive spectroscopy (EDS). The  $\tau_f$  of  $(1-x)\text{Zn}_2\text{SiO}_4-x\text{CaTiO}_3$  was found to be dependent on phase constitution, which is related to the amount of  $\text{CaTiO}_3$ . When  $x=0.05$ , the  $\tau_f$  of  $(1-x)\text{Zn}_2\text{SiO}_4-x\text{CaTiO}_3$  was near 0 ppm/°C. The microwave dielectric properties of  $0.95\text{Zn}_2\text{SiO}_4-0.05\text{CaTiO}_3$  ceramics samples with  $\text{Li}_2\text{CO}_3$ – $\text{H}_3\text{BO}_3$  additives sintered at 900–1000 °C were characterized, and the results indicated that the permittivity and  $Q \times f$  were associated with the amount of  $\text{Li}_2\text{CO}_3$ – $\text{H}_3\text{BO}_3$  and the sintering temperature. The sintering temperature of ceramics was effectively reduced to 950 °C from about 1250 °C and the temperature coefficient of resonant frequency ( $\tau_f$ ) was modified to  $-4.5$  ppm/°C with good  $Q \times f$ . The addition of 4.0 wt%  $\text{Li}_2\text{CO}_3$ – $\text{H}_3\text{BO}_3$  in  $0.95\text{Zn}_2\text{SiO}_4-0.05\text{CaTiO}_3$  ceramics sintered at 950 °C showed excellent dielectric properties of  $\epsilon_r=7.1$ ,  $Q \times f=26,300$  GHz ( $f=7.1$  GHz) and  $\tau_f=-4.5$  ppm/°C. Moreover, this material has a chemical compatibility with silver, making it a very promising candidate material for LTCC applications.

© 2011 Published by Elsevier B.V.

## 1. Introduction

The rapid progress in microwave telecommunication and satellite broadcasting has resulted in an increasing demand for microwave dielectric materials. Low-temperature co-fired ceramics (LTCC) have been widely investigated as a means of miniaturizing microwave devices. For practical application in microwave dielectric materials as substrates or patch antennas in LTCC, the materials must display low permittivity, high quality factor ( $Q \times f$ ), a near zero temperature coefficient of resonant frequency ( $\tau_f \sim 0$  ppm/°C) and a low-firing temperature (<961 °C, the melting temperature of Ag electrode) [1–8]. Most commercial LTCC materials have relative permittivity less than 10 and the lowest loss tangent values close to 0.0002 at microwave frequencies. A new-glass-ceramics (NGC) that consists of  $\text{MgAl}_2\text{O}_4$  crystals (spinel) and highly crystallized Li–Mg–Zn–B–Si–O glass has been developed by Murata Manufacturing for microwave or millimeter-wave frequency applications [9]. The KAI Multilayer Division of Kyocera America, Inc. utilizes both the Ferro A6 and DuPont LTCC materials for use in these demanding Multi-Chip Modules.

Willemite ( $\text{Zn}_2\text{SiO}_4$ ) ceramics as silicates are proposed as good candidates for millimeter-wave dielectrics because of their low  $\epsilon_r$  of 6.6 and high  $Q \times f$  value of 219,000 GHz [10]. But the large negative  $\tau_f$  of  $-61$  ppm/°C and high sintering temperatures (>1300 °C) could put constraints on their application as substrate materials. In order to adjust the  $\tau_f$  value to zero,  $\text{TiO}_2$  ( $\tau_f \sim +450$  ppm/°C) was added. A near zero  $\tau_f$  value ( $\tau_f=1.0$  ppm/°C) can be obtained by adding 11 wt%  $\text{TiO}_2$  [10]. However, it required a sintering temperatures as high as 1250 °C. For practical application in LTCC, it is necessary to lower the sintering temperature of the ceramics.

There are three methods to reduce the sintering temperature of microwave dielectric ceramics: first, low melting oxide, mixture oxide or glass addition; second, chemical processing; and finally the use of smaller particles as the starting materials [11–21]. The chemical method is time-consuming and expensive. Pamu et al. found that  $\text{B}_2\text{O}_3$  could effectively decrease the sintering temperature of  $(\text{Zr}_{0.8}\text{Sn}_{0.2})\text{TiO}_4$  to 1150 °C from 1650 °C [22]. In our previous work, it was found that the addition of  $\text{BaCu}(\text{B}_2\text{O}_5)$  lowered the sintering temperature of  $\text{ZnTiNb}_2\text{O}_8$  ceramics from above 1250 °C to 950 °C [23]. Li et al. could successfully reduce the sintering temperature of  $(\text{Zn}_{0.65}\text{Mg}_{0.35})\text{TiO}_3$ – $\text{CaTiO}_3$  ceramics from 1150 °C to 950 °C by using  $\text{CaO}$ – $\text{B}_2\text{O}_3$ – $\text{SiO}_2$  additive, and adjust  $\tau_f$  by doping  $\text{CaTiO}_3$  [24]. Generally, the addition of low melting point materials such as  $\text{B}_2\text{O}_3$ ,  $\text{CuO}$ ,  $\text{Bi}_2\text{O}_3$ ,  $\text{V}_2\text{O}_5$  and  $\text{Li}_2\text{CO}_3$  is known to be the most effective

\* Corresponding author. Tel.: +86 27 8754 5167; fax: +86 27 8754 5167.  
E-mail address: [dxzhou@mail.hust.edu.cn](mailto:dxzhou@mail.hust.edu.cn) (D. Zhou).

and cheap way to achieve dense sintered ceramics at low sintering temperature.

In this paper, attempts were made to achieve a near-zero  $\tau_f$  of  $\text{Zn}_2\text{SiO}_4$ , and to lower the sintering temperature below  $950^\circ\text{C}$ . Since  $\text{Zn}_2\text{SiO}_4$  ceramics have negative  $\tau_f$  values and  $\text{CaTiO}_3$  has a  $\tau_f$  of  $+859\text{ ppm}/^\circ\text{C}$ ,  $\varepsilon_r$  of 162 and  $Q \times f$  value of 12,960 GHz [25,26], the  $(1-x)\text{Zn}_2\text{SiO}_4-x\text{CaTiO}_3$  composite ceramics should have adjustable  $\tau_f$  values. In  $(1-x)\text{Zn}_2\text{SiO}_4-x\text{CaTiO}_3$  composite ceramics ( $x=0.05$ ), the sintering temperature was lowered below  $950^\circ\text{C}$  by adding  $\text{Li}_2\text{CO}_3\text{-H}_3\text{BO}_3$  as a sintering aid. The effects of densification, crystalline phases and microstructure on the microwave dielectric properties of  $\text{Zn}_2\text{SiO}_4$  ceramics were explored.

## 2. Experimental procedures

Both  $\text{Zn}_2\text{SiO}_4$  and  $\text{CaTiO}_3$  compounds were individually synthesized by conventional solid-state reaction method using reagent-grade powders:  $\text{ZnO}$  (99.6%),  $\text{SiO}_2$  (99.7%),  $\text{CaCO}_3$  (99.5%) and  $\text{TiO}_2$  (99.6%). For the preparation of  $\text{Zn}_2\text{SiO}_4$  and  $\text{CaTiO}_3$  compounds, the high-purity raw materials were weighed according to the desired stoichiometry and ball-milled in a polyethylene jar containing zirconia balls with ethanol for 4 h. After drying at  $80^\circ\text{C}$ , the mixed powders were individually ground and then calcined at  $1200^\circ\text{C}$  for 3 h and  $1100^\circ\text{C}$  for 2 h in air. The compounds were individually re-milled for 4 h to obtain the desired composition:  $(1-x)\text{Zn}_2\text{SiO}_4-x\text{CaTiO}_3$  ( $x=0, 0.01, 0.02, 0.03, 0.04, 0.05, 0.06$  and  $0.07$ ) and  $0.95\text{Zn}_2\text{SiO}_4-0.05\text{CaTiO}_3$  doped with 2.0, 3.0, 4.0, 5.0 and 6.0 wt%  $\text{Li}_2\text{CO}_3\text{-H}_3\text{BO}_3$ . Then the mixed powders were dried, granulated and pressed into several disk-type pellets (25 mm in diameter and 15 mm in thickness). The  $(1-x)\text{Zn}_2\text{SiO}_4-x\text{CaTiO}_3$  ( $x=0-0.07$ ) pellets were sintered at  $1200-1300^\circ\text{C}$  for 3 h and the  $0.95\text{Zn}_2\text{SiO}_4-0.05\text{CaTiO}_3$  pellets containing 2.0–6.0 wt%  $\text{Li}_2\text{CO}_3\text{-H}_3\text{BO}_3$  were sintered at  $900-1000^\circ\text{C}$  for 3 h in air.

Crystalline phases of the sintered samples were identified by X-ray diffraction (XRD: PANalytical B.V., X'Pert PRO) using  $\text{Cu K}\alpha$  radiation, the microstructures were studied using scanning electron microscope (SEM: Philip, XL30TM) and composition analysis was performed using energy-dispersive spectroscopy (EDS: EDAX, PHOENIX). The bulk densities of the sintered ceramics were measured using the Archimedes method. The microwave dielectric properties were measured by an Advantest network analyzer (E5071C). The  $\varepsilon_r$  and  $Q$  values were measured by using the Hakki-Coleman dielectric resonator method [27,28]. The temperature coefficient of resonant frequency ( $\tau_f$ ) was also measured by the same method using Eq. (1)

$$\tau_f \text{ (ppm}/^\circ\text{C}) = \frac{(f_{80} - f_{25}) \times 10^6}{55f_{25}} \quad (1)$$

where  $f_{80}$  and  $f_{25}$  are the resonant frequencies at  $80^\circ\text{C}$  and  $25^\circ\text{C}$ , respectively.

## 3. Results and discussion

Fig. 1 shows the X-ray powder diffraction (XRD) patterns of  $(1-x)\text{Zn}_2\text{SiO}_4-x\text{CaTiO}_3$  ( $x=0.03-0.07$ ) ceramic samples at the fixed sintering temperature of  $1250^\circ\text{C}$  for 3 h in air. All the

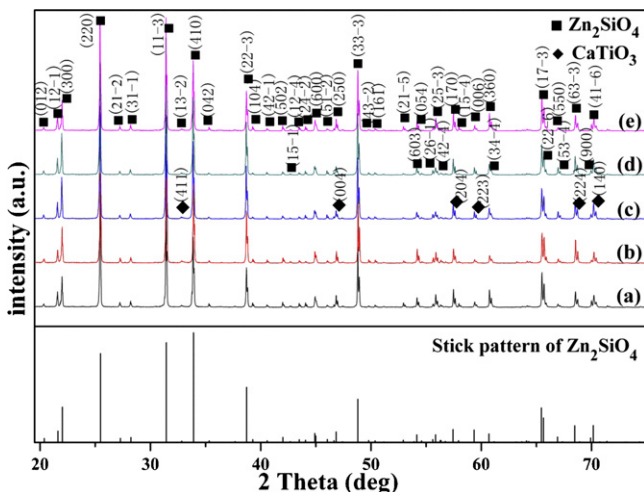


Fig. 1. XRD patterns of  $(1-x)\text{Zn}_2\text{SiO}_4-x\text{CaTiO}_3$  ceramics (a)  $x=0.03$ , (b)  $x=0.04$ , (c)  $x=0.05$ , (d)  $x=0.06$  and (e)  $x=0.07$  sintered at  $1250^\circ\text{C}$  for 3 h in air.

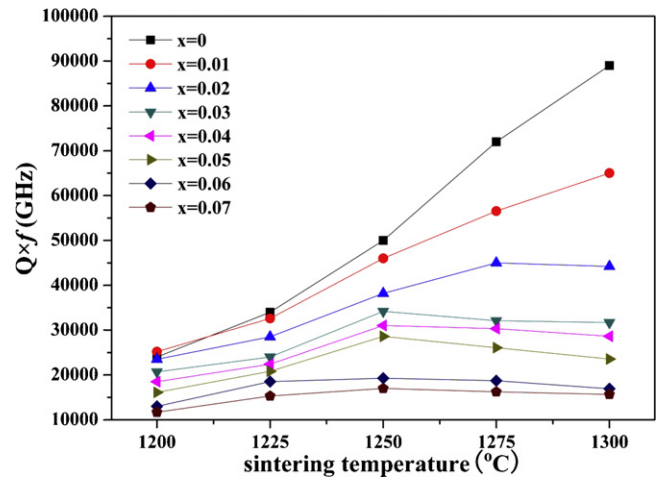


Fig. 2. The  $Q \times f$  of  $(1-x)\text{Zn}_2\text{SiO}_4-x\text{CaTiO}_3$  ( $x=0, 0.01, 0.02, 0.03, 0.04, 0.05, 0.06$  and  $0.07$ ) ceramics sintered at  $1200^\circ\text{C}$ ,  $1225^\circ\text{C}$ ,  $1250^\circ\text{C}$ ,  $1275^\circ\text{C}$  and  $1300^\circ\text{C}$  for 3 h in air.

compounds exhibit the mixture of  $\text{Zn}_2\text{SiO}_4$  (JCPDS #72-1856) and  $\text{CaTiO}_3$  (JCPDS #82-0231). The peaks indicated the presence of  $\text{Zn}_2\text{SiO}_4$  as the main crystalline phase, and  $\text{CaTiO}_3$  as the minor crystalline phase.  $\text{Zn}_2\text{SiO}_4$  belongs to the rhombohedral crystal system (space group  $R-3$  (no. 148)), and the lattice parameters are  $a=b=13.9720\text{ \AA}$ ,  $c=9.3340\text{ \AA}$ .  $\text{CaTiO}_3$  belongs to the orthorhombic crystal system (space group  $Pbnm$  (no. 62)), and the lattice parameters are  $a=5.4642\text{ \AA}$ ,  $b=5.4804\text{ \AA}$ ,  $c=7.7452\text{ \AA}$ .

Fig. 2 shows the  $Q \times f$  values of  $(1-x)\text{Zn}_2\text{SiO}_4-x\text{CaTiO}_3$  ( $x=0-0.07$ ) ceramics sintered at  $1200-1300^\circ\text{C}$  for 3 h in air. The  $Q \times f$  value of samples decreased gradually with increasing  $\text{CaTiO}_3$  content.  $\text{Zn}_2\text{SiO}_4$  has a higher  $Q \times f$  value of 219,000 GHz, and  $\text{CaTiO}_3$  has a lower  $Q \times f$  of 12,960 GHz [9,16]. Consequently, when the  $\text{CaTiO}_3$  content increased, the  $Q \times f$  values of the compounds decreased gradually due to its relatively lower  $Q \times f$  value. However, when  $x=0, 0.01$  or  $0.02$ , the  $Q \times f$  value of  $(1-x)\text{Zn}_2\text{SiO}_4-x\text{CaTiO}_3$  ceramic samples increased with increasing sintering temperature. The ceramics may not have been sintering enough at  $1200-1300^\circ\text{C}$ , because of the high sintering temperatures of  $\text{Zn}_2\text{SiO}_4$  (more than  $1350^\circ\text{C}$ ). When  $x=0.03-0.07$ , the  $Q \times f$  value of  $(1-x)\text{Zn}_2\text{SiO}_4-x\text{CaTiO}_3$  ceramic samples first increased with the sintering temperature to a maximum value at  $1250^\circ\text{C}$  and then decreased at higher temperature. The decrease in  $Q \times f$  at temperature higher than  $1250^\circ\text{C}$  may have been as a result of oversintering. These also proved that the addition of  $\text{CaTiO}_3$  can decrease the sintering temperature of  $\text{Zn}_2\text{SiO}_4$  ceramics.

Table 1 shows that the theoretical and the measured permittivity  $\varepsilon_r$  and  $\tau_f$  values of  $(1-x)\text{Zn}_2\text{SiO}_4-x\text{CaTiO}_3$  ( $x=0-0.07$ ) ceramics sintered at  $1250^\circ\text{C}$  for 3 h. The theoretical permittivities of the composite ceramic were obtained from the well-known Lichtenecker empirical rule [29].

$$\log \varepsilon = V_1 \log \varepsilon_1 + V_2 \log \varepsilon_2 \quad (2)$$

where  $V_1$  and  $V_2$  are the volume fractions;  $\varepsilon_1$  and  $\varepsilon_2$  are the permittivities of the  $\text{Zn}_2\text{SiO}_4$  ceramic and the  $\text{CaTiO}_3$  ceramic, respectively. The measured permittivity of the  $(1-x)\text{Zn}_2\text{SiO}_4-x\text{CaTiO}_3$  composite ceramic agreed well with the theoretical value (Table 1). It increased from 6.6 to 9.9 as the  $x$  value increased from 0 to 0.07.

The temperature coefficient of resonant frequency ( $\tau_f$ ) can be obtained from the thermal expansion coefficient  $\alpha_L$  and the temperature coefficient of permittivity  $\tau_\varepsilon$  as follows:

$$\tau_f = -\alpha_L - \frac{1}{2\tau_\varepsilon} \quad (3)$$

**Table 1**  
Permittivity  $\varepsilon_r$  and  $\tau_f$  of  $(1-x)\text{Zn}_2\text{SiO}_4-x\text{CaTiO}_3$  ( $x=0-0.07$ ) composite ceramics sintered at 1250 °C for 3 h in air.

Compounds	$\varepsilon_r$ (theo.)	$\varepsilon_r$ (meas.)	$\tau_f$ (theo.) (ppm/°C)	$\tau_f$ (meas.) (ppm/°C)
$x=0$ [9]		6.6		-61.0
$x=0.01$	6.7	6.7	-54.9	-52.0
$x=0.02$	6.9	6.8	-48.8	-43.5
$x=0.03$	7.0	7.1	-42.6	-31.5
$x=0.04$	7.2	7.2	-36.3	-17.7
$x=0.05$	7.4	8.2	-30.0	+0.8
$x=0.06$	7.5	9.1	-23.7	+15.8
$x=0.07$	7.7	9.9	-17.3	+28.6

$\varepsilon_r$  (theo.): theoretical permittivity;  $\varepsilon_r$  (meas.): measured permittivity.

$\tau_f$  (theo.): theoretical  $\tau_f$  value;  $\tau_f$  (meas.): measured  $\tau_f$  value.

The  $\tau_\varepsilon$  is defined as the following:

$$\tau_\varepsilon = V_1 \tau_{\varepsilon 1} + V_2 \tau_{\varepsilon 2} \quad (4)$$

where  $V_1$  and  $V_2$  are the volume fraction of  $\text{Zn}_2\text{SiO}_4$  and  $\text{CaTiO}_3$ . According to the Lichtenecker empirical rule, the mixing rule of  $\tau_f$  can be described like this:

$$\tau_f = V_1 \tau_{f1} + V_2 \tau_{f2} \quad (5)$$

where  $\tau_{f1}$  and  $\tau_{f2}$  are the  $\tau_f$  values of the  $\text{Zn}_2\text{SiO}_4$  and  $\text{CaTiO}_3$  phase, respectively. The theoretical  $\tau_f$  values of the  $(1-x)\text{Zn}_2\text{SiO}_4-x\text{CaTiO}_3$  composite ceramics were calculated using the function (5). The  $\tau_f$  values results were listed in Table 1. The measured  $\tau_f$  was somewhat positive compared to the theoretical value. This might result from the element diffusion in the  $(1-x)\text{Zn}_2\text{SiO}_4-x\text{CaTiO}_3$  compounds. When the  $\text{CaTiO}_3$  increased from 0 mol% to 7.0 mol%, the  $\tau_f$  value of the sample increased from -61.0 ppm/°C to +28.6 ppm/°C.  $\text{Zn}_2\text{SiO}_4$  has a lower  $\tau_f$  of -61.0 ppm/°C, and  $\text{CaTiO}_3$  has a higher  $\tau_f$  of +859 ppm/°C [10,25]. Consequently, when the  $\text{CaTiO}_3$  content increased, the  $\tau_f$  value of the sample increased gradually. A near zero  $\tau_f$  value ( $\tau_f=0.8$  ppm/°C) can be obtained in  $0.95\text{Zn}_2\text{SiO}_4-0.05\text{CaTiO}_3$  compounds sintering at 1250 °C for 3 h in air.

The XRD patterns of  $0.95\text{Zn}_2\text{SiO}_4-0.05\text{CaTiO}_3$  ceramic samples with 2.0–6.0 wt%  $\text{Li}_2\text{CO}_3-\text{H}_3\text{BO}_3$  additives sintered at 950 °C for 3 h are shown in Fig. 3. Fig. 4 shows the XRD patterns of  $0.95\text{Zn}_2\text{SiO}_4-0.05\text{CaTiO}_3$  ceramic samples with 4.0 wt%  $\text{Li}_2\text{CO}_3-\text{H}_3\text{BO}_3$  additives sintered at different temperatures (900–1000 °C) for 3 h in air. The XRD patterns showed that the samples contained three phases: the first is  $\text{Zn}_2\text{SiO}_4$  (JCPDS #72-1856), the second is  $\text{CaTiO}_3$  (JCPDS #82-0231) and the third phase.

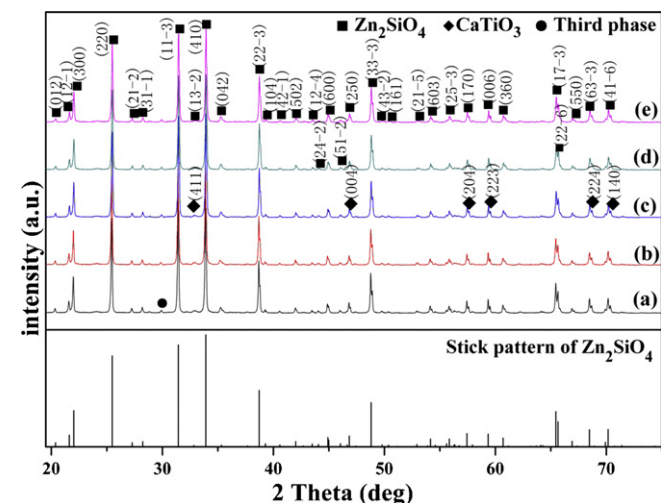


**Fig. 3.** XRD patterns of  $0.95\text{Zn}_2\text{SiO}_4-0.05\text{CaTiO}_3$  ceramics with (a) 2.0 wt%, (b) 3.0 wt%, (c) 4.0 wt%, (d) 5.0 wt% and (e) 6.0 wt%  $\text{Li}_2\text{CO}_3-\text{H}_3\text{BO}_3$  additives sintered at 950 °C for 3 h in air.

Unfortunately, the third phase has not been identified. The XRD patterns of the  $0.95\text{Zn}_2\text{SiO}_4-0.05\text{CaTiO}_3$  ceramic did not change markedly with the sintering temperatures in the range of 900–1000 °C or the increasing  $\text{Li}_2\text{CO}_3-\text{H}_3\text{BO}_3$  content from 2.0 wt% to 6.0 wt%.

The SEM micrographs of the  $0.95\text{Zn}_2\text{SiO}_4-0.05\text{CaTiO}_3$  ceramics with different wt% of  $\text{Li}_2\text{CO}_3-\text{H}_3\text{BO}_3$  additive (2.0–6.0 wt%) sintered at 950 °C for 3 h are shown in Fig. 5(a)–(e). The grains got more and more dense with the increasing  $\text{Li}_2\text{CO}_3-\text{H}_3\text{BO}_3$  content. However, when the  $\text{Li}_2\text{CO}_3-\text{H}_3\text{BO}_3$  content was more than 4.0 wt%, abnormal grain growth was observed. The SEM micrographs of  $0.95\text{Zn}_2\text{SiO}_4-0.05\text{CaTiO}_3$  samples with 4.0 wt%  $\text{Li}_2\text{CO}_3-\text{H}_3\text{BO}_3$  sintered at different temperature (900–1000 °C) are presented in Fig. 6(a)–(e). It can be seen that the grains became larger and denser with increasing sintering temperature.

In order to analyze the composition, the EDS of  $0.95\text{Zn}_2\text{SiO}_4-0.05\text{CaTiO}_3$  samples with 4.0 wt%  $\text{Li}_2\text{CO}_3-\text{H}_3\text{BO}_3$  sintered at 950 °C for 3 h is shown in Fig. 7. The results indicated the ratio of Zn:Si:O of spot A is about 2:1:4, which is consistent with the composition of  $\text{Zn}_2\text{SiO}_4$ . And the ratio of Ca:Ti:O of spot B is about 1:1:3, which is also consistent with the composition of  $\text{CaTiO}_3$ . These supported the results of XRD which showed that the samples contained two separate phases of  $\text{Zn}_2\text{SiO}_4$  and  $\text{CaTiO}_3$ . It seems impossible to detect lithium and boron ions using an EDS detector, meaning that the  $\text{Li}_2\text{CO}_3-\text{H}_3\text{BO}_3$  could not be detected. However, the  $\text{Li}_2\text{CO}_3-\text{H}_3\text{BO}_3$  has been successfully applied as a sintering aid to enhance the sintering properties of the  $0.95\text{Zn}_2\text{SiO}_4-0.05\text{CaTiO}_3$  ceramics, as shown in Figs. 5 and 9(a).

The XRD pattern and BSEM micrograph of the  $0.95\text{Zn}_2\text{SiO}_4-0.05\text{CaTiO}_3$  ceramics with 4.0 wt%  $\text{Li}_2\text{CO}_3-\text{H}_3\text{BO}_3$

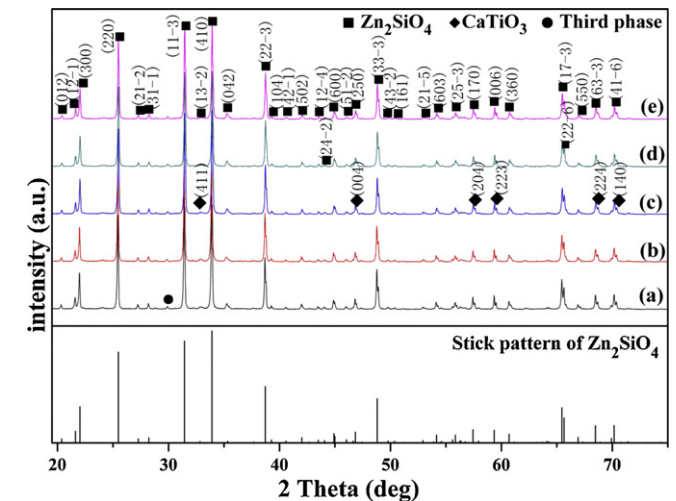


**Fig. 4.** XRD patterns of  $0.95\text{Zn}_2\text{SiO}_4-0.05\text{CaTiO}_3$  ceramics with 4.0 wt%  $\text{Li}_2\text{CO}_3-\text{H}_3\text{BO}_3$  additives sintered at (a) 900 °C, (b) 925 °C, (c) 950 °C, (d) 975 °C and (e) 1000 °C for 3 h in air.

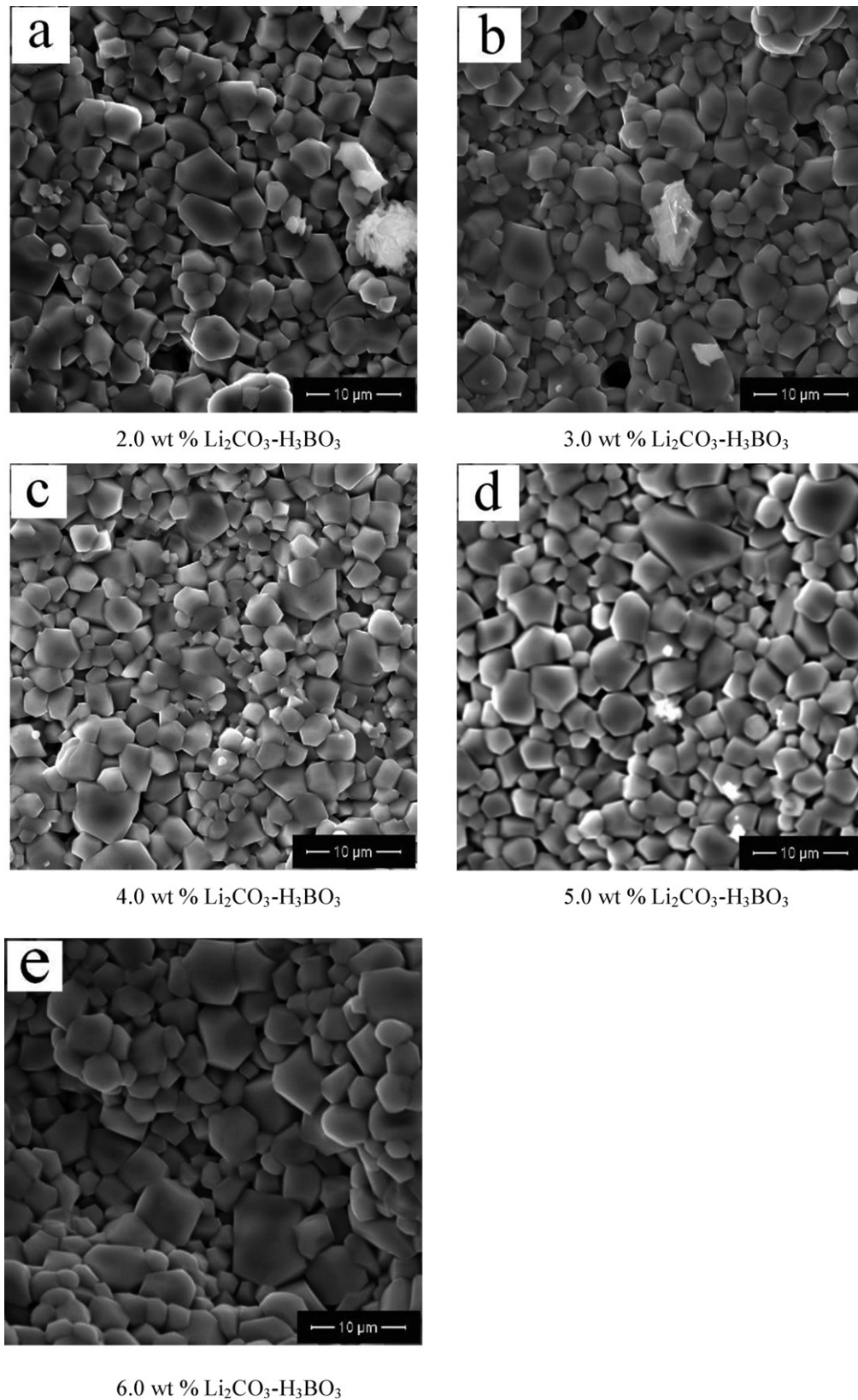


**Fig. 5.** SEM micrographs of  $0.95\text{Zn}_2\text{SiO}_4\text{-}0.05\text{CaTiO}_3$  ceramics with (a) 2.0 wt%, (b) 3.0 wt%, (c) 4.0 wt%, (d) 5.0 wt% and (e) 6.0 wt%  $\text{Li}_2\text{CO}_3\text{-H}_3\text{BO}_3$  additives sintered at  $950^\circ\text{C}$  for 3 h in air.

and 20.0 wt% Ag addition sintered at  $950^\circ\text{C}$  for 3 h are shown in Fig. 8. All the major peaks of Ag are observed in the XRD pattern and no phase containing silver compounds was present. In the BSEM micrograph, pale Ag particles have a uniform distribution in the

ceramic and do not react with it. Therefore the composite exhibits chemical compatibility with Ag electrodes and the co-firing of Ag electrodes with the  $0.95\text{Zn}_2\text{SiO}_4\text{-}0.05\text{CaTiO}_3$  ceramics is possible.

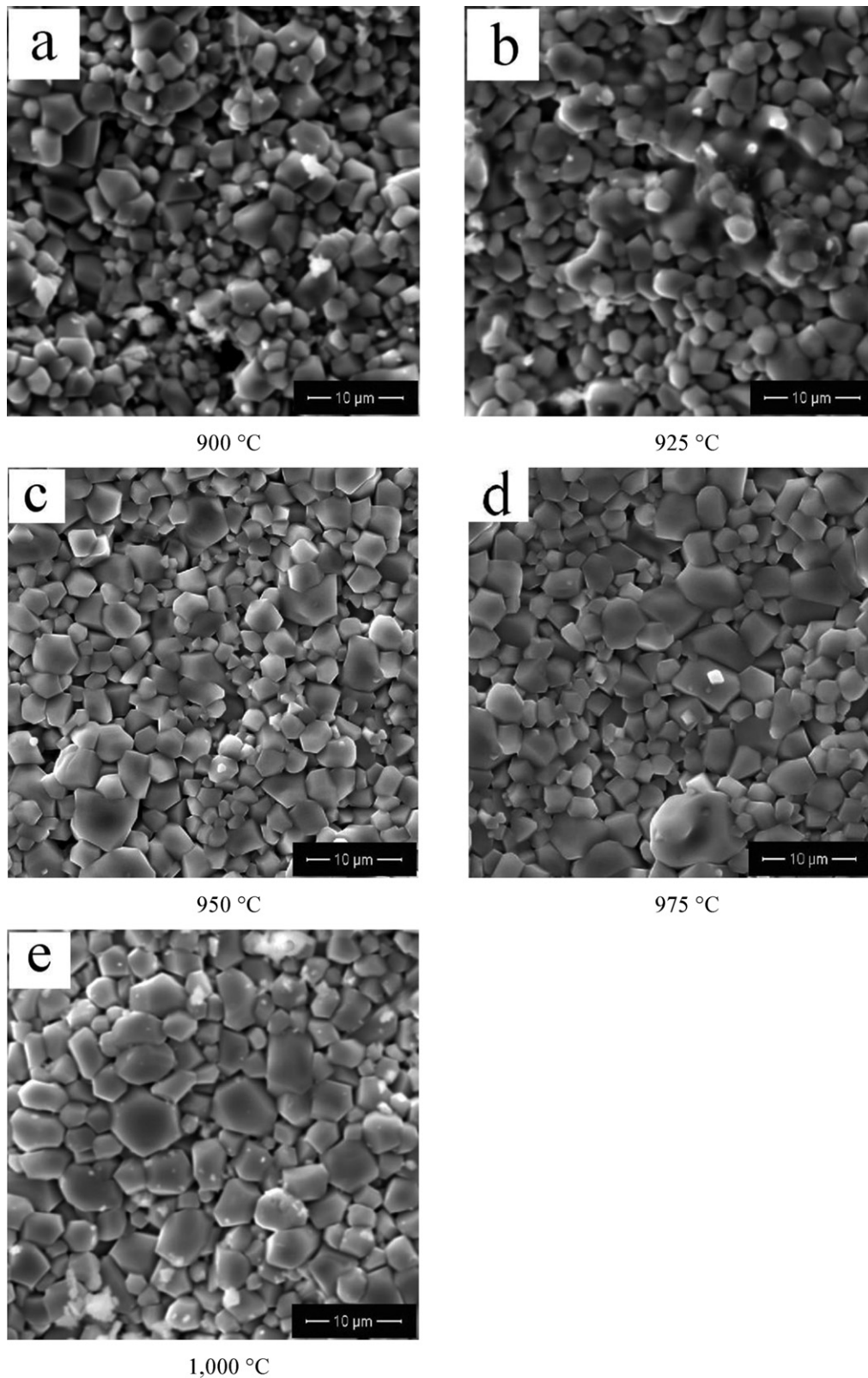


**Fig. 6.** SEM micrographs of  $0.95\text{Zn}_2\text{SiO}_4-0.05\text{CaTiO}_3$  ceramics with 4.0 wt%  $\text{Li}_2\text{CO}_3-\text{H}_3\text{BO}_3$  additives sintered at (a) 900 °C, (b) 925 °C, (c) 950 °C, (d) 975 °C and (e) 1000 °C for 3 h in air.

**Fig. 9(a)** shows the relative density of  $0.95\text{Zn}_2\text{SiO}_4-0.05\text{CaTiO}_3$  ceramic samples with 2.0–6.0 wt%  $\text{Li}_2\text{CO}_3-\text{H}_3\text{BO}_3$  sintered at 900–1000 °C for 3 h in air. The relative density of the samples increased with the increasing sintering temperature due to the

decrease in the porosity and the increase of the grain sizes. However, when the sintering temperature was above 950 °C, the relative densities of samples of more than 4.0 wt%  $\text{Li}_2\text{CO}_3-\text{H}_3\text{BO}_3$  were almost invariable and at over 94% of the theoretical density, which

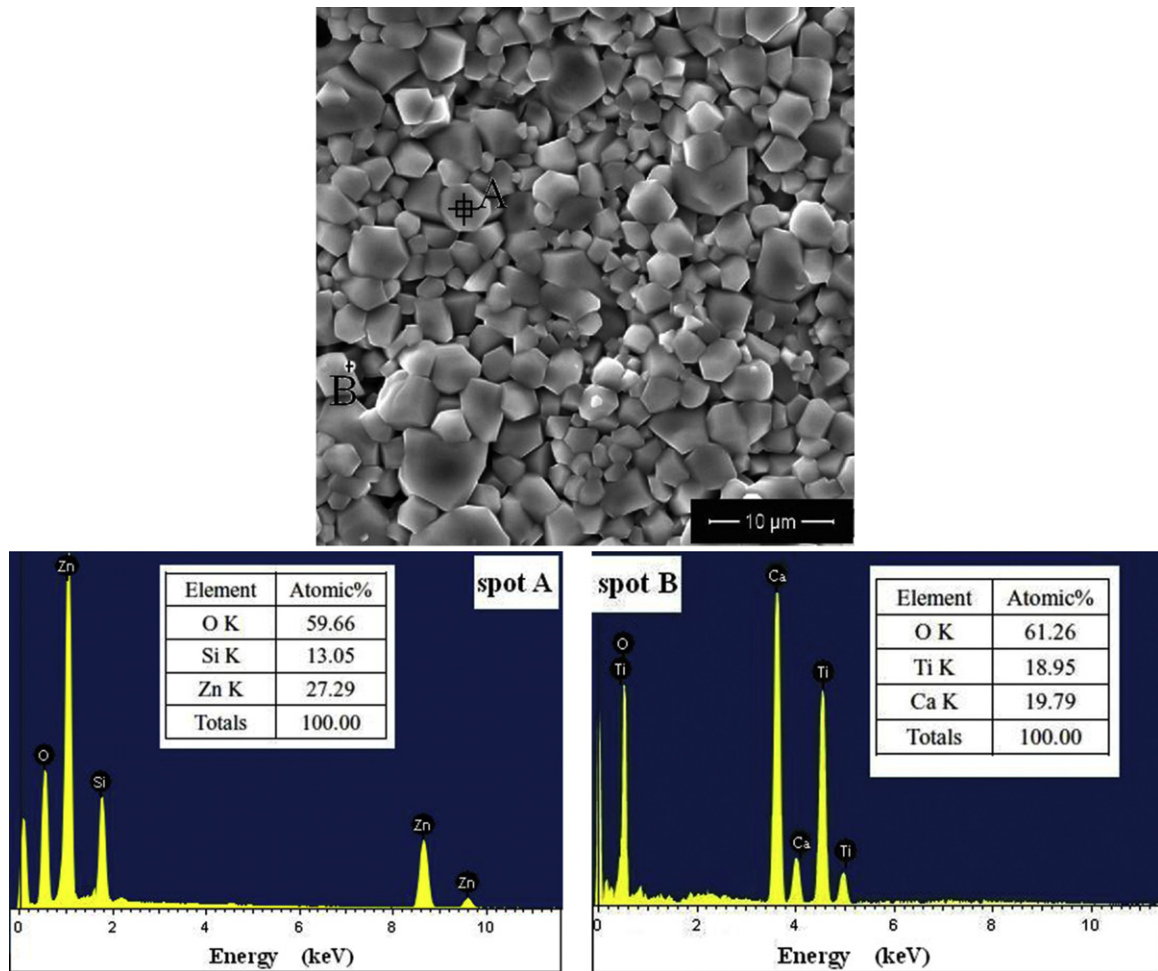


Fig. 7. EDS analysis of  $0.95\text{Zn}_2\text{SiO}_4-0.05\text{CaTiO}_3$  samples with 4.0 wt%  $\text{Li}_2\text{CO}_3-\text{H}_3\text{BO}_3$  additives sintered at  $950^\circ\text{C}$  for 3 h in air.

indicated that the samples with 4.0 wt%  $\text{Li}_2\text{CO}_3-\text{H}_3\text{BO}_3$  which were sintered above  $950^\circ\text{C}$  were very dense as shown in Fig. 6(c)–(e).

Fig. 9(b) and (c) shows the permittivity  $\epsilon_r$  and  $Q \times f$  values of  $0.95\text{Zn}_2\text{SiO}_4-0.05\text{CaTiO}_3$  ceramic samples with 2.0–6.0 wt%  $\text{Li}_2\text{CO}_3-\text{H}_3\text{BO}_3$  sintered at  $900-1000^\circ\text{C}$  for 3 h in air. It can be seen that the permittivity  $\epsilon_r$  and density showed a similar trend with

the increasing temperature and  $\text{Li}_2\text{CO}_3-\text{H}_3\text{BO}_3$  content, because densification of the ceramics plays an important role in influencing the permittivity  $\epsilon_r$  [30]. Fig. 9(c) shows that the  $Q \times f$  values first increased and then decreased with the increase of the  $\text{Li}_2\text{CO}_3-\text{H}_3\text{BO}_3$  content and sintering temperature, and the  $Q \times f$  values of the ceramic samples reached a maximum value at  $950^\circ\text{C}$

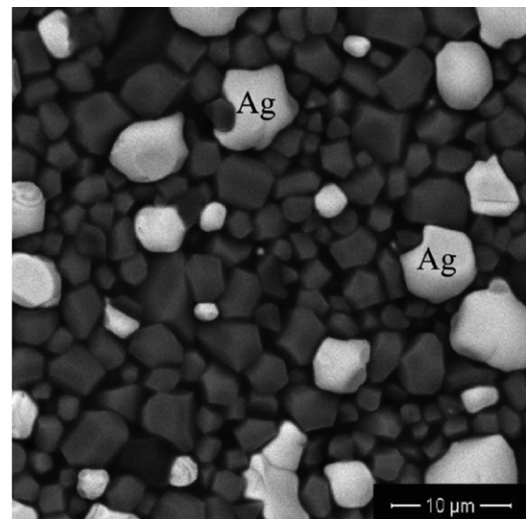
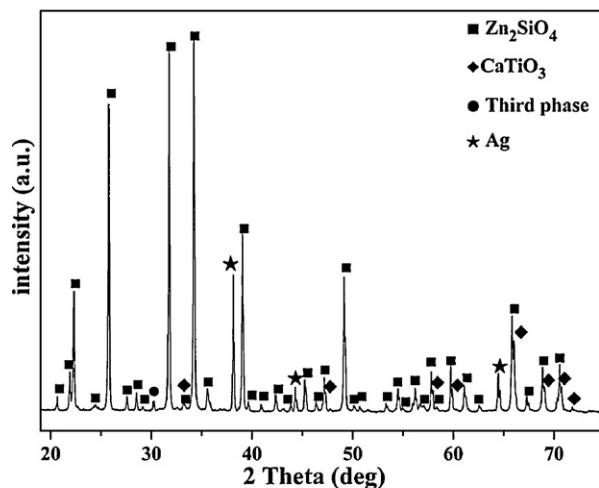


Fig. 8. XRD pattern and BSEM micrograph of  $0.95\text{Zn}_2\text{SiO}_4-0.05\text{CaTiO}_3$  ceramics with 4.0 wt%  $\text{Li}_2\text{CO}_3-\text{H}_3\text{BO}_3$  and 20.0 wt% Ag addition sintered at  $950^\circ\text{C}$  for 3 h in air.

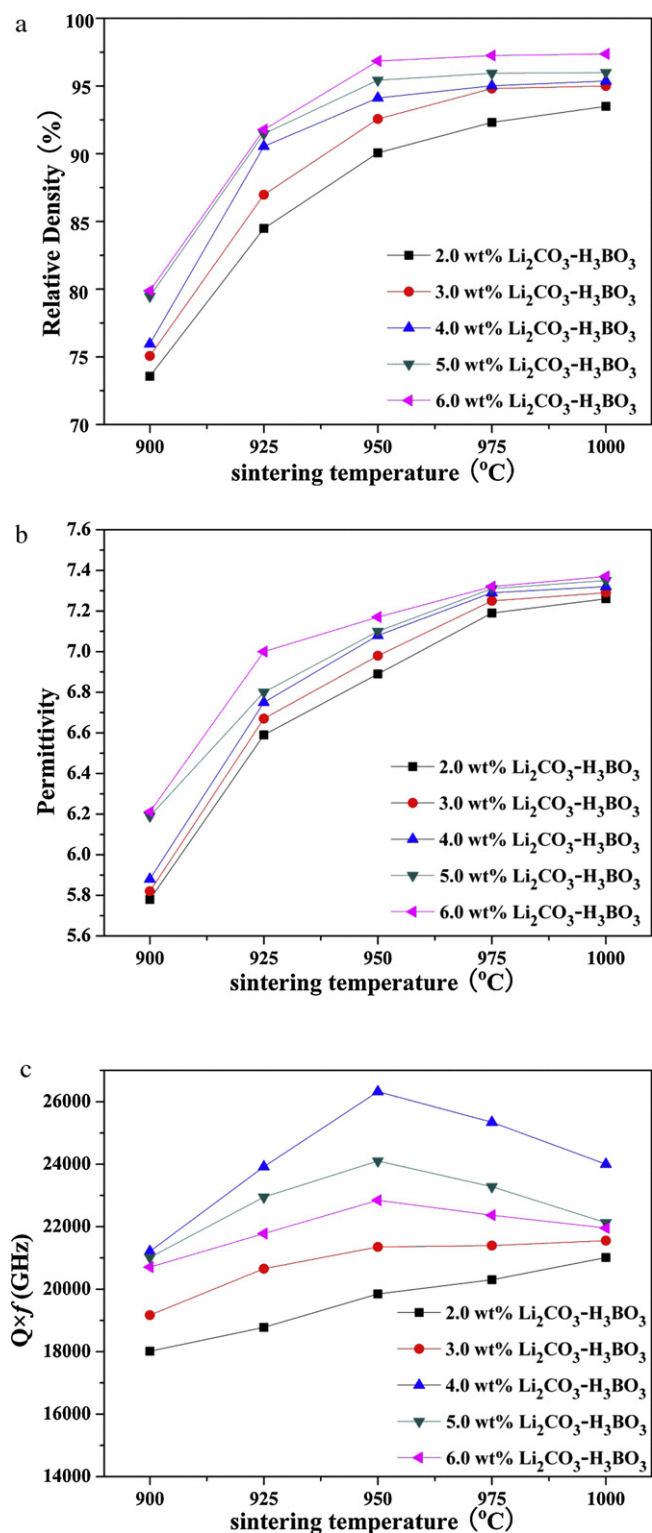


Fig. 9. (a) The relative density, (b) the permittivity and (c) the  $Q \times f$  of  $0.95\text{Zn}_2\text{SiO}_4-0.05\text{CaTiO}_3$  ceramics with 2.0, 3.0, 4.0, 5.0 and 6.0 wt% of  $\text{Li}_2\text{CO}_3-\text{H}_3\text{BO}_3$  additives sintered at 900 °C, 925 °C, 950 °C, 975 °C and 1000 °C for 3 h in air.

when 4.0 wt%  $\text{Li}_2\text{CO}_3-\text{H}_3\text{BO}_3$  was added. As the grains became more and more dense with increasing  $\text{Li}_2\text{CO}_3-\text{H}_3\text{BO}_3$  content as shown in Fig. 5(a)–(e), the  $Q \times f$  values were expected to increase. However, the  $Q \times f$  values decreased when the  $\text{Li}_2\text{CO}_3-\text{H}_3\text{BO}_3$  content was more than 4.0 wt%. It might be related to abnormal growth of the grains, as their grain sizes were as large as 10  $\mu\text{m}$  as shown in

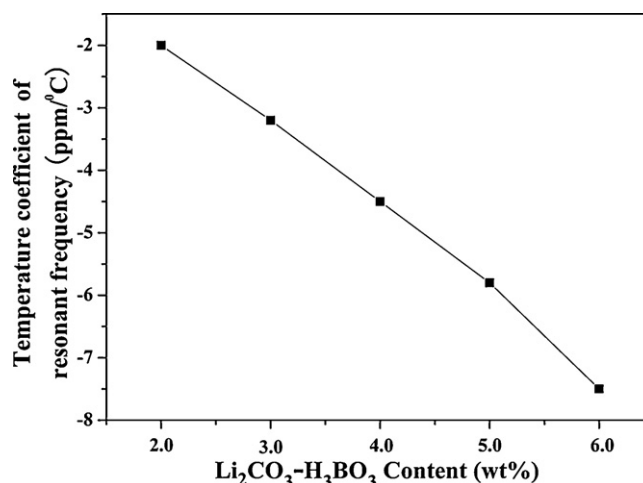


Fig. 10. The  $\tau_f$  of  $0.95\text{Zn}_2\text{SiO}_4-0.05\text{CaTiO}_3$  ceramics with 2.0, 3.0, 4.0, 5.0 and 6.0 wt% of  $\text{Li}_2\text{CO}_3-\text{H}_3\text{BO}_3$  addition sintered at 950 °C for 3 h in air.

Fig. 5(d) and (e). Therefore, the addition of 4.0 wt% of  $\text{Li}_2\text{CO}_3-\text{H}_3\text{BO}_3$  is the optimum way that we found to enhance the microwave dielectric properties of the material. The effectiveness of sintering aids was very much affected by the sintering temperatures [31]. According to Fig. 9(c), the  $Q \times f$  values of the sample doped with 4.0 wt%  $\text{Li}_2\text{CO}_3-\text{H}_3\text{BO}_3$  reached the maximum when the sintering temperature was as high as 950 °C. It also may be because the samples had high density and homogenous grain size at 950 °C. From XRD results in Fig. 4 and SEM observations in Fig. 6(a)–(e), phases and peak intensity remained almost unchanged for the compounds with 4.0 wt% of  $\text{Li}_2\text{CO}_3-\text{H}_3\text{BO}_3$  regardless of sintering temperature, but densification and grain sizes increased with the increasing sintering temperature. According to the classical dielectric theory, the  $Q$  value should increase as the grain size increases, because a reduction in the number of grain boundaries per unit volume would result in a material with a lower loss [32]. In fact, the samples had the highest  $Q \times f$  value when the average grain sizes of the samples was about 2–5  $\mu\text{m}$  as shown in Figs. 5(c) and 6(c). Alford et al. [32] also observed similar results for alumina, and in our previous work [33],  $\text{ZnTiNb}_2\text{O}_8$  with  $\text{BaCu}(\text{B}_2\text{O}_5)$  display similar behavior which is in contrast to classical theory. This may be as a result of the interaction of many factors, such as grain size, porosity or presence of liquid-phase, which made it difficult to give definitive remarks on grain size–loss relationships [32]. Therefore, we cannot make practical use of the grain size–loss relationships in this case [33].

Fig. 10 shows the  $\tau_f$  value of  $0.95\text{Zn}_2\text{SiO}_4-0.05\text{CaTiO}_3$  ceramics with 2.0–6.0 wt%  $\text{Li}_2\text{CO}_3-\text{H}_3\text{BO}_3$  additives sintered at 950 °C for 3 h in air. The  $\tau_f$  decreased slightly with an increase of  $\text{Li}_2\text{CO}_3-\text{H}_3\text{BO}_3$  content, changing from  $-2.0 \text{ ppm}/^\circ\text{C}$  to  $-7.5 \text{ ppm}/^\circ\text{C}$ . The third phase was observed when the  $\text{Li}_2\text{CO}_3-\text{H}_3\text{BO}_3$  addition was doped to  $(1-x)\text{Zn}_2\text{SiO}_4-x\text{CaTiO}_3$  ceramic samples, but not observed in pure  $(1-x)\text{Zn}_2\text{SiO}_4-x\text{CaTiO}_3$  samples. The slight decrease in  $\tau_f$  with the increase of  $\text{Li}_2\text{CO}_3-\text{H}_3\text{BO}_3$  content may be related to this third phase. A low temperature coefficient of the resonant frequency ( $\tau_f \sim 0 \text{ ppm}/^\circ\text{C}$ ) is one of the most important properties for microwave dielectric materials in LTCC applications. We have achieved  $\tau_f = -4.5 \text{ ppm}/^\circ\text{C}$  when  $0.95\text{Zn}_2\text{SiO}_4-0.05\text{CaTiO}_3$  compounds were doped with 4.0 wt% of  $\text{Li}_2\text{CO}_3-\text{H}_3\text{BO}_3$ .

#### 4. Conclusions

In this work, the temperature coefficient of resonant frequency ( $\tau_f$ ) of  $\text{Zn}_2\text{SiO}_4$  was adjusted by doping with  $\text{CaTiO}_3$  at 1250 °C, and  $\text{Li}_2\text{CO}_3-\text{H}_3\text{BO}_3$  additives were used as sintering

aids to effectively lower the sintering temperature of the material. The temperature coefficient of resonant frequency ( $\tau_f$ ) was found to be dependent on phase constitutions, which is in turn related to the amount of  $\text{CaTiO}_3$  present. When  $x=0.05$ , the  $\tau_f$  of  $(1-x)\text{Zn}_2\text{SiO}_4-x\text{CaTiO}_3$  approached 0 ppm/°C. The dielectric properties of  $0.95\text{Zn}_2\text{SiO}_4-0.05\text{CaTiO}_3$  samples with  $\text{Li}_2\text{CO}_3-\text{H}_3\text{BO}_3$  additives sintered at 900–1000 °C were investigated, and the results indicated that the behaviors of the permittivity and  $Q \times f$  were associated with the amount of  $\text{Li}_2\text{CO}_3-\text{H}_3\text{BO}_3$  and the sintering temperature. As a result, the sintering temperature of the ceramics was effectively reduced to 950 °C from above 1250 °C and the temperature coefficient of resonant frequency ( $\tau_f$ ) was successfully modified to  $-4.5$  ppm/°C with good  $Q \times f$ . Addition of 4.0 wt%  $\text{Li}_2\text{CO}_3-\text{H}_3\text{BO}_3$  to  $0.95\text{Zn}_2\text{SiO}_4-0.05\text{CaTiO}_3$  ceramics sintered at 950 °C showed excellent dielectric properties of  $\epsilon_r = 7.1$ ,  $Q \times f = 26,300$  GHz ( $f = 7.1$  GHz) and  $\tau_f = -4.5$  ppm/°C. Moreover, the material was compatible with Ag electrodes, making it a very promising candidate material for LTCC applications.

## References

- [1] C.L. Huang, C.L. Pan, W.C. Lee, J. Alloys Compd. 462 (2008) L5–L8.
- [2] J. Wang, Z. Yue, Z. Gui, L. Li, J. Alloys Compd. 392 (2005) 263–267.
- [3] R. Umemura, H. Ogawa, A. Yokoi, H. Ohsato, A. Kan, J. Alloys Compd. 424 (2006) 388–393.
- [4] D.K. Kwon, M.T. Lanagan, T.R. Shrout, J. Am. Ceram. Soc. 88 (2005) 3419–3422.
- [5] D. Chu, L. Fang, H. Zhou, X. Chen, Z. Yang, J. Alloys Compd. 509 (2011) 1931–1935.
- [6] H.K. Shin, H. Shin, S.Y. Cho, K.S. Hong, J. Am. Ceram. Soc. 88 (2005) 2461–2465.
- [7] P.S. Anjana, T. Joseph, M.T. Sebastian, J. Alloys Compd. 490 (2010) 208.
- [8] M.T. Sebastian, Dielectric Materials for Wireless Communication, Elsevier Science, Oxford, UK, 2008.
- [9] N. Mori, Y. Sugimoto, J. Harada, Y. Higuchi, J. Eur. Ceram. Soc. 26 (2006) 1925–1928.
- [10] Y. Guo, H. Ohsato, K.I. Kakimoto, J. Eur. Ceram. Soc. 26 (2006) 1827–1830.
- [11] S. George, M.T. Sebastian, J. Alloys Compd. 473 (2009) 336–340.
- [12] Y.B. Chen, J. Alloys Compd. 509 (2011) 6884–6888.
- [13] H. Zhou, X. Liu, H. Wang, X. Chen, H. Zhou, Ceram. Int. (2011), doi:10.1016/j.ceramint.2011.07.015.
- [14] H. Naghib-zadeh, C. Glitzky, W. Oesterle, T. Rabe, J. Eur. Ceram. Soc. 31 (2011) 589–596.
- [15] L. Fang, D. Chu, H. Zhou, X. Chen, Z. Yang, J. Alloys Compd. 509 (2011) 1880–1884.
- [16] L. Wang, J.J. Bian, Mater. Lett. 65 (2011) 726–728.
- [17] C. Nam, H. Park, I. Seo, J. Choi, S. Nahm, H. Lee, J. Alloys Compd. 509 (2011) 3686–3689.
- [18] O. Renoult, J.P. Boilot, F. Chaput, R. Papiernik, L.G. Hubert-Pfalzgraf, J. Am. Ceram. Soc. 75 (1992) 3337–3340.
- [19] M. Zhang, H. Wang, H. Yang, X. Wu, W. Liu, X. Yao, J. Alloys Compd. 509 (2011) L344–L347.
- [20] M.H. Liang, S.Y. Wu, C.T. Hu, I.N. Li, Mater. Chem. Phys. 79 (2003) 276–281.
- [21] J.S. Kim, M.E. Song, M.R. Joung, J.H. Choi, S. Nahm, S.I. Gu, J.H. Paik, B.H. Choi, J. Eur. Ceram. Soc. 30 (2010) 375–379.
- [22] D. Pamu, G. Lakshmi Narayana Rao, K.C. James Rajua, J. Alloys Compd. 509 (2011) 9289–9295.
- [23] D. Zhou, G. Dou, M. Guo, S. Gong, Mater. Chem. Phys. 130 (2011) 903–908.
- [24] B. Li, X.H. Zhou, S.R. Zhang, L.C. Xiang, Key Eng. Mater. 235 (2010) 434–435.
- [25] P.L. Wise, I.M. Reaney, W.E. Lee, T.J. Price, D.M. Iddles, D.S. Cannell, J. Eur. Ceram. Soc. 21 (2001) 2629–2632.
- [26] C.L. Huang, J.Y. Chen, G.S. Huang, J. Alloys Compd. 499 (2010) 48–52.
- [27] B.W. Hakki, P.D. Coleman, IEEE Trans. Micro. Theory Tech. 8 (1960) 402–410.
- [28] W.E. Courtney, IEEE Trans. Micro. Theory Tech. 18 (1970) 476–485.
- [29] Y.G. Wu, X.H. Zhao, F. Li, Z.G. Fan, J. Electroceram. 11 (2003) 227–239.
- [30] C.F. Tseng, H.J. Tang, J. Alloys Compd. 491 (2010) 314–318.
- [31] J.H. Jeon, S.C. Lin, J. Am. Ceram. Soc. 83 (2000) 1417–1422.
- [32] S.J. Penn, N.M. Alford, A. Templeton, X. Wang, M. Xu, M. Reece, K. Schrapel, J. Am. Ceram. Soc. 80 (1997) 1885–1888.
- [33] M. Guo, S. Gong, G. Dou, D. Zhou, J. Alloys Compd. 509 (2011) 5988–5995.